JOURNAL OF MATERIALS SCIENCE 12 (1977) 2099–2108

Local stress and strain during crack growth by steady state creep

J. T. BARNBY
Department of Metallurgy and Materials, University of Aston, Birmingham, UK

R. D. NICHOLSON
Central Electricity Generating Board, Berkeley Nuclear Laboratories, Berkeley, Gloucestershire, UK

Experimental methods are used to measure the distribution of plastic strain ahead of a crack propagating under steady state creep conditions. Using these strains the local strain-rates are known, and from these the steady state stress distribution is deduced assuming power law behaviour. The resulting information indicates that the stress distribution is closer to $\sigma_{ss} \propto x^{-1/(m+1)}$ than to $\sigma_{ss} \propto x^{-1/(2m)}$. It is shown that for low values of the exponent, m, in the power law, that creep crack growth should correlate with the elastic stress intensity factor, whereas at large m values a better correlation is expected with the net stress.

1. Introduction

In the interests of operational safety of engineering plant and the design of plant operating at high temperatures, it is necessary to have a foundation for design against the growth of creep cracks. Theories of triple point cracking [1] and cavitation at grain boundaries [2] are well developed, but explain only the micromechanics operating in the region of stress and strain concentration at the tip of a macrocrack. The engineering requirement is a description of how a macro-creep-crack would lead to failure of an engineering structure.

Historically, theories of failure by creep have encompassed geometrical features of cracking into the mathematical formulation of a 'damage' function [3]. Such theories are quire successful and have recently been extended by more detailed treatment of material behaviour in the crack tip vicinity [4]. Other theories have developed in analogous ways to yielding theory, using such concepts as a 'reference stress' [5]. The size and physical location of the reference stress is then used to allow for all geometrical phenomena and the final failure considered to be equivalent to that of a uniaxial stress-rupture test piece.

In such work the details of cracking are entirely omitted, but allowed for somehow in the phenomenology. There is a danger that by avoiding explicit treatment of the moving crack that similar problems, to those in brittle fracture, may be encountered before the mechanics of fracture were well understood. It therefore seems of value to pursue the explicit treatment of crack advance under creep conditions.

Early work by Wells [6] indicated that creep-crack growth was susceptible to treatment using fracture mechanics parameters. Subsequently empirical correlations were established between the rate of creep-crack growth, da/dt, and the elastic stress intensity factor K [7, 8]. In cases where the exponent m in the creep rate relation has large values, the correlation with K could not be established, though a good empirical correlation between da/dt and the net section stress was evident [9]. It has been shown [10] that both of these laws arise as special cases if the creep-crack growth rate is controlled by the crack-tip local stresses. When $m = 1$, that is for a viscous material obeying Newton's law, application of the Hoff analogy [11] gives a crack-tip stress distribution

analogous to that in linear elastic behaviour, though of course the behaviour is far from elastic. When m has values of 7 or more, the steady state crack-tip stresses fall much more rapidly with distance down to the net section stress. Thus the transmission from a K-controlled to a net section stress-controlled cracking rate can be explained simply as a function of m.

Materials with K-controlled cracking rates have come to be called "creep brittle", while those with net stress control are called "creep ductile". However, it would seem inappropriate to propagate this terminology since it seems likely that either type of material could have high or low ductility in principle, though fortuitous correlations may arise. Indeed the case of $m = 1$ would appear to give K-control, though such a material behaviour is often associated with superplasticity.

2. Theoretical considerations

Making the usual five assumptions [3] concerning the behaviour of metals during secondary creep (namely; incompressibility, creep rate independent of hydrostatic stresses, existence of a flow potential, isotropic behaviour, applicability of Norton's Law for uniaxial tests) and strain rate tensor v_{ij} is:

$$v_{ij} = \frac{d\varepsilon_{ij}}{dt} = \frac{3}{2}\left(\frac{\sigma_e}{\sigma_c}\right)^{m-1}\frac{S_{ij}}{\sigma_c} \quad (1)$$

Here σ_e is the effective stress, σ_c is a material property and S_{ij} arises from the deviatoric stress tensor [3]. Thus concentrating on the v_{11}, and writing in terms of principal stresses $\sigma_1, \sigma_2, \sigma_3$,

$$\frac{d\varepsilon_{11}}{dt} = \frac{B}{2^{(m+1)/2}}[(\sigma_1-\sigma_2)^2+(\sigma_2-\sigma_3)^2 + (\sigma_3-\sigma_1)^2]^{(m-1)/2} [(\sigma_1-\sigma_2)-(\sigma_3-\sigma_1)] \quad (2)$$

Here the σ_c property has been incorporated into the property B following Pao and Marin [12].

Further narrowing considerations to those of plane stress conditions ($\sigma_3 = \sigma_{23} = \sigma_{13} = 0$) and to the region ahead of a slit crack, we find, according to polar co-ordinates with the origin at the crack tip,

$$\sigma_1 = \frac{K_I}{(2\pi r)^{1/2}}\cos\frac{\theta}{2}\left[1+\sin\frac{\theta}{2}\sin\frac{3\theta}{2}\right]+\ldots$$

$$\sigma_2 = \frac{K_I}{(2\pi r)^{1/2}}\cos\frac{\theta}{2}\left[1-\sin\frac{\theta}{2}\sin\frac{3\theta}{2}\right]+\ldots$$

$$\sigma_{12} = \frac{K_I}{(2\pi r)^{1/2}}\sin\frac{\theta}{2}\cos\frac{\theta}{2}\cos\frac{3\theta}{2}+\ldots \quad (3)$$

Here K_I is the mode I elastic stress intensity factor. With $\theta = 0, r = x$ on the cracking plane:

$$\sigma_1 = \frac{K_I}{(2\pi x)^{1/2}}$$

Hence under relaxation by power law creep we have from Equation 2,

$$\frac{d\varepsilon_{11}}{dt} = \dot{\varepsilon}_1 = \frac{B}{2}(\sigma_1)^m = \frac{B}{2}(\sigma_y)^m \quad (4)$$

Here the ordinate y has origin at the crack tip.

If a given critical displacement in the y direction is an adequate criterion for crack tip advance then we can deal simply with σ_y and ε_y connected by the power law creep equation.

In an earlier paper [14] an approximate method was used to obtain the steady state values of $\sigma_y(x)$ following viscous relaxation of the elastic distribution of stresses which would exist in the absence of creep. The relaxation of the elastic stresses given by

$$\sigma_y = \frac{K_I}{(2\pi x)^{1/2}}$$

was considered to be a transient at a fixed total strain. This elastic strain converts to plastic strain by time dependent viscous flow as in Fig. 1. Following the transient, which is known to be rapid [15], the stress reaches a steady state value, σ_{ss}, such that the strain $\varepsilon(x)$ is:

$$\varepsilon(x) = A\sigma_{ss}^m. \quad (5)$$

If almost all the elastic strain is converted to plastic viscous strain then the elastic strain, $K/E(2\pi x)^{1/2}$ is approximately:

$$\frac{K}{E(2\pi x)^{1/2}} = A\sigma_{ss}^m \quad (6)$$

This fixes the relaxed stress distribution such that

$$\sigma_{ss} \propto x^{-1/2m}. \quad (7)$$

Though this relaxation at constant total strain seems plausible during a rapid creep transient, and the final dominance of creep strain over elastic strain is a prerequisite for application of Hoff's analogy, the resulting stress distribution is not consistent with the work of Rice and Rosengren [16] and of Hutchinson [17]. These authors base their stress distribution, following plastic flow, on the

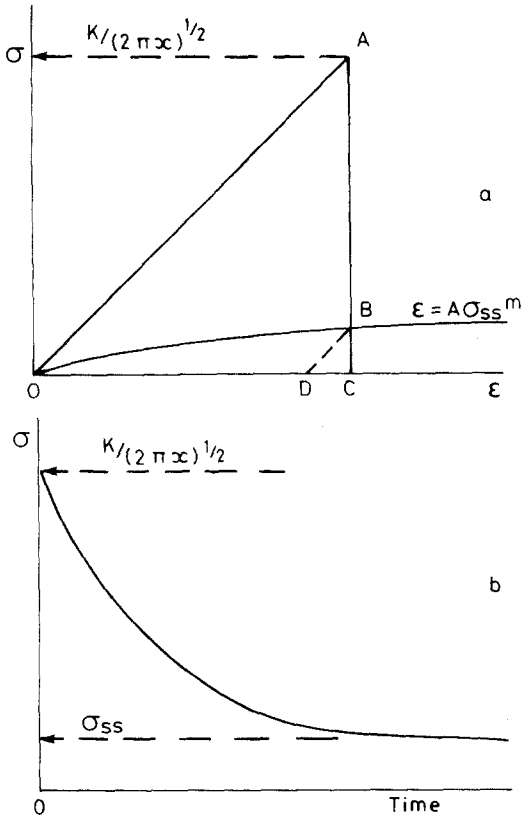

Figure 1 (a) Relaxation of the local stress σ from the linear elastic value at A to the steady state value at B. The residual elastic strain DC is much less than the viscous strain OC. (b) Local stress relaxation versus time.

assumption that the elastic strain energy density must have an exact $1/x$ variation as the crack tip is approached no matter what material behaviour occurs.

Using the Hoff analogy through an energy argument we can use the plasticity and creep rate power laws:

$$\varepsilon = B\sigma^m, \quad \dot{\varepsilon} = B\sigma^m.$$

The complementary energy U for an element ahead of the crack tip would be

$$U = \int \varepsilon \mathrm{d}\sigma = \int B\sigma^m \mathrm{d}\sigma = \frac{B}{m+1}\sigma^{m+1} \quad (8)$$

If all products of the type $\varepsilon\sigma$ must have a $1/x$ singularity at the crack tip, no matter what stress–strain law operates, then U has such a singularity. Going to the total complementary energy U_T, by integrating throughout the volume V,

$$U_T = \int U \mathrm{d}V = \int \frac{B}{m+1}\sigma_{ij}^{m+1}\mathrm{d}V \quad (9)$$

The σ_{ij} steady state values can be arrived at by use of a variational theorem such that

$$\frac{\mathrm{d}U_T}{\mathrm{d}\sigma_{ss}} = \frac{\mathrm{d}\left\{\int\left[\frac{B}{m+1}\sigma_{ij}^{(m+1)}\mathrm{d}V\right]\right\}}{\mathrm{d}\sigma_{ss}} = 0. \quad (10)$$

Here only the σ_{ij} depends on x and so $\sigma_{ij}^{m+1}(x)$ must be proportional to $1/x$ thus:

$$\sigma_{ss} \propto x^{-1/(m+1)}. \quad (11)$$

Further, following this unproven assumption [16] that there must always be a $1/x$ singularity in strain energy, then the local strains must show a dependence on $x^{-m/(m+1)}$.

Equivalent to the assumption of the $1/x$ strain energy singularity is the Neuber rule [18] for concentrated stresses with plastic deformation taking place. At each point ahead of the crack tip we can imagine the stress to fall from the hypothetical linear elastic value by relaxing down the hyperbola $\sigma\varepsilon = Q^2$. Then as in Fig. 2 we have:

$$\sigma_E \varepsilon_E = \sigma_{ss}\varepsilon_{ss}$$

Relaxation occurs down to the intersection with the power law $\varepsilon = A\sigma_{ss}^m$ which is the analogy of $\dot{\varepsilon} = A\sigma_{ss}^m$. Since

$$\sigma_E = \frac{K}{(2\pi x)^{1/2}},$$

then

$$\sigma_{ss} = \left(\frac{K^2}{2\pi EA}\right)^{1/(m+1)} x^{-1/(m+1)}.$$

Since both of the models for the profile of steady state stress are built on assumptions and approximations it seems appropriate to verify

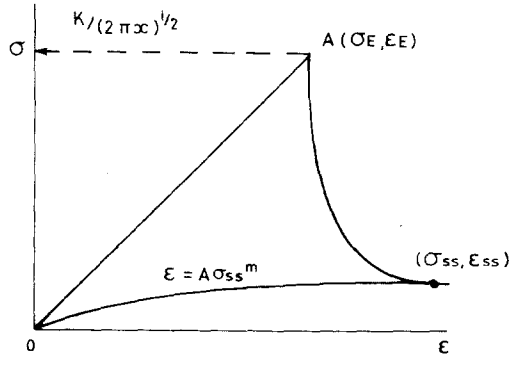

Figure 2 Relaxation of elastic stress by plastic deformation according to Neuber.

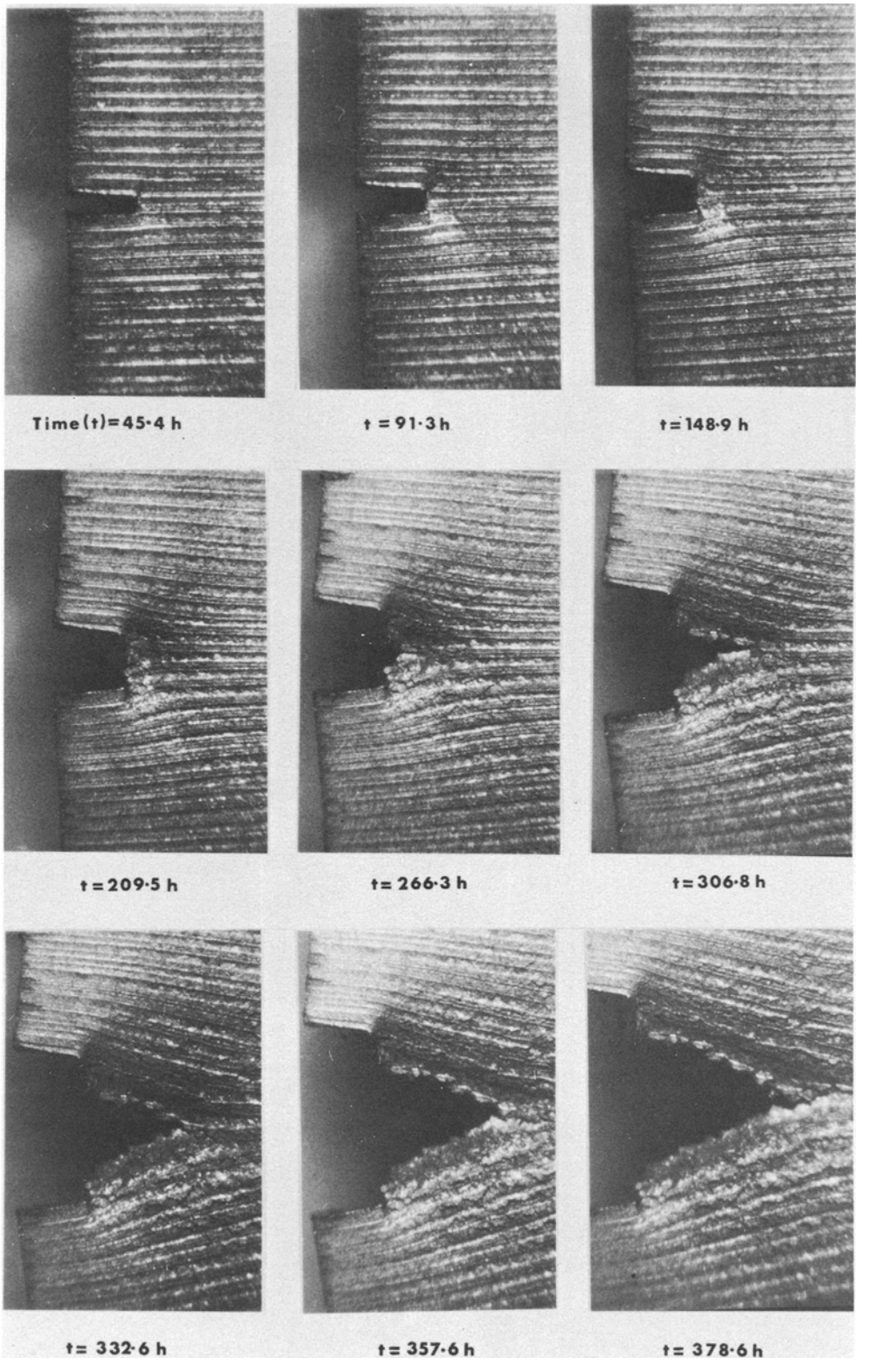

Figure 3 Creep-crack growth in type 316 steel at 650° C, X 20. ($\dot{\delta} = 1.2 \times 10^{-5}$ m h^{-1}).

actual material behaviour experimentally. Accordingly, experiments were carried out on AISI 316 stainless steel under plane stress conditions thus avoiding the currently unpredictable plane strain effects.

A previous model [10] to predict the rate of growth of a creep crack da/dt related to the cracking rate to the crack-tip stress distribution dependent of $x^{-1/2m}$. The model predicted the experimentally observed dependence of da/dt on K for small m, but on σ_{net} for large m. In the appendix, it is shown that similar behaviour will occur if the crack tip steady state stresses depend on $x^{-1/(m+1)}$.

3. Experimental methods and materials

Specimens were cut from AISI 316 steel strip 50 mm wide and 0.75 mm thick. The strip had been 20% reduced cold. The composition of the steel in wt % was

C	Mn	Si	S	P
0.06	1.79	0.51	0.018	0.023
Ni	Cr	Mo	Fe	
11.72	17.82	2.76	balance.	

The specimens were 10 mm x 0.75 mm x 150 mm and double edge notches 0.7 mm deep were cut in the middle of the specimens. The specimens were sealed in an evacuated capsule and heat-treated at 1050 ± 1° C for 1 h, then air-cooled. The resulting grain size was 33 μm using the linear intercept method. Specimens were ground to a 6 μm diamond paste finish and finally scratch-marks spaced approximately 0.1 mm apart were made parallel to and covering the region of the notches.

These specimens were tested in a modified Hounsfield tensometer at a constant crosshead displacement rate. During straining the specimens were enclosed in a vacuum chamber located on the Hounsfield tensometer and viewed through a window of optically flat silica in the vacuum chamber. Heating was by a resistance furnace with a circular viewing port, constructed by winding 87/14 platinum/rhodium wire on a fused alumina cylinder and employing tantalum radiation shields. During testing the central 25 mm of the test piece varied in temperature by less than 5° C.

The specimen was viewed through a Zeiss microscope with a long focal length objective, positioned over the vacuum chamber and photographs taken by a cine camera with a 5 min time lapse setting. Tests were carried out at 650° and 750° C with cross-head speeds of 1.2×10^{-5} m h^{-1} or 1.1×10^{-4} m h^{-1}. After a primary region in which the load increased with strain the load became steady and the conditions were then equivalent to those of steady state creep. The time, t_s, to reach a constant load condition was determined from a load–time recording and thus the positions of scribe lines were known from photographs at the onset of the constant load region and at successive intervals.

Creep cracking did not initiate immediately from the notch, though the initiation time t_i was greater than t_s. Measurements of the displacement of scribe lines from the onset of steady state conditions were taken using a gauge length of three line spacings. Thus from the known time under steady state conditions local strain rates could be deduced.

4. Experimental results

Photographs illustrating the strain measurement method are shown in Fig. 3. To ensure that the local strains were in fact uniform over the gauge lengths chosen, the displacement, y, of each line from the cracking plane at points ahead of the notch at time t_s was measured. At a later time t_2 ($< t_i$), the displacements were remeasured and the additional displacements, $u = (Y_{t_2} - Y_{t_s})$ were calculated. A typical result is shown in Fig. 4, where displacements only one side of the plane are shown since the situation is symmetrical. All gauge lengths used were within the range where displacements are linear with distance and the strain therefore uniform.

Fig. 5 shows the strain rates derived from the distribution of strains ahead of the creep crack propagating under steady state conditions at 750° C. Strain distributions measured after 162.7, 182.7 and 199.2 h, superimpose, demonstrating the steady state, though there is a change after 228.5 h when the influence of the free boundary to which the crack is propagating may begin to be felt.

The logarithmic co-ordinates emphasise the region R immediately ahead of the crack tip where the strain rate is approximately constant reflecting a region of constant stress. Beyond this the strain rate distribution reflects the stress profile which levels out as the net stress level is reached.

Steady state strain rates were used to deduce stresses assuming power law creep, $\dot{\varepsilon} = A\sigma^m$,

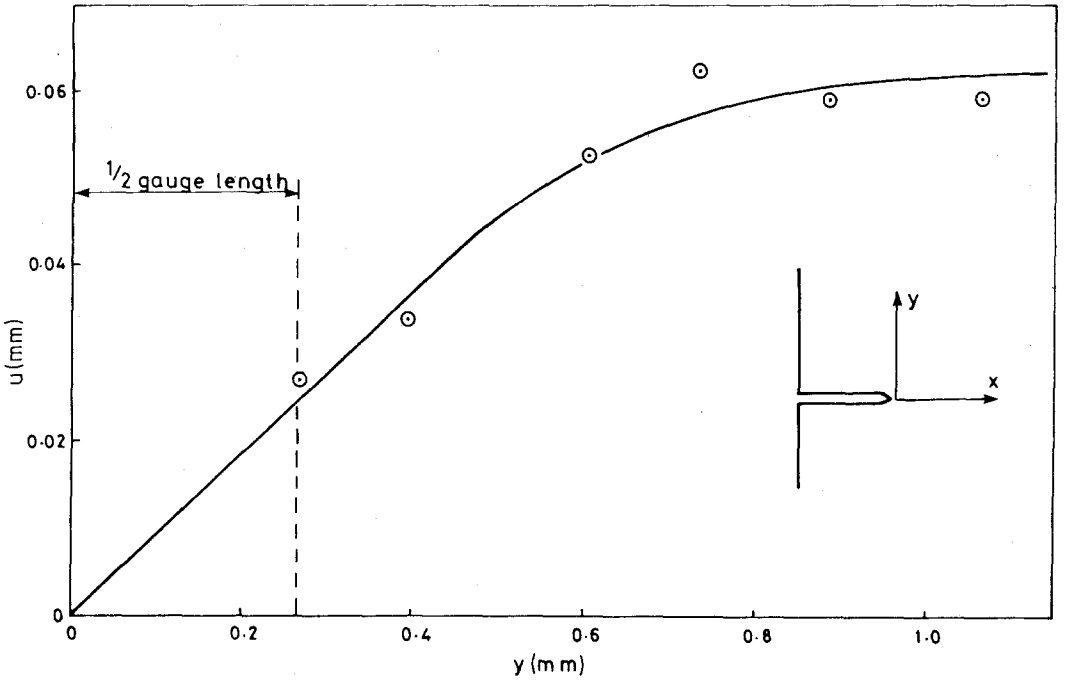

Figure 4 Example of the variation of displacement u in the y direction versus distance in the y direction. Measurements taken 0.14 mm ahead of the crack tip.

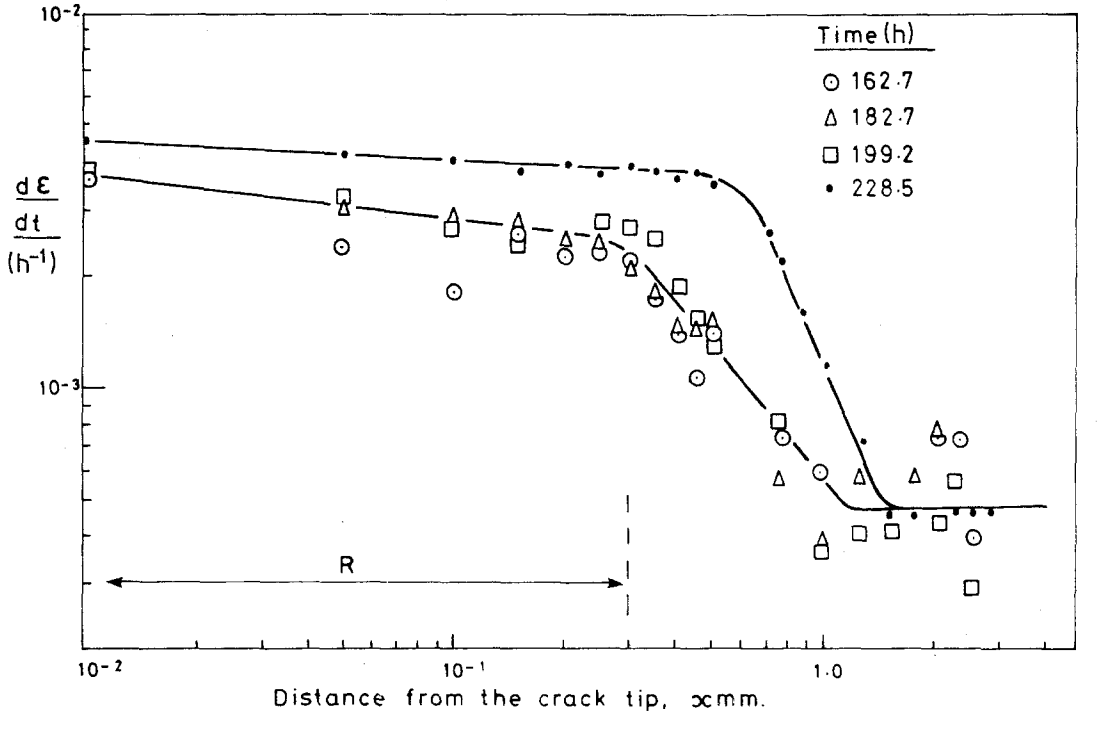

Figure 5 Steady state strain rates measured versus distance x from the crack tip after times shown for test at 750° C and displacement rate $\dot{\delta} = 1.2 \times 10^{-5}$ m h^{-1}.

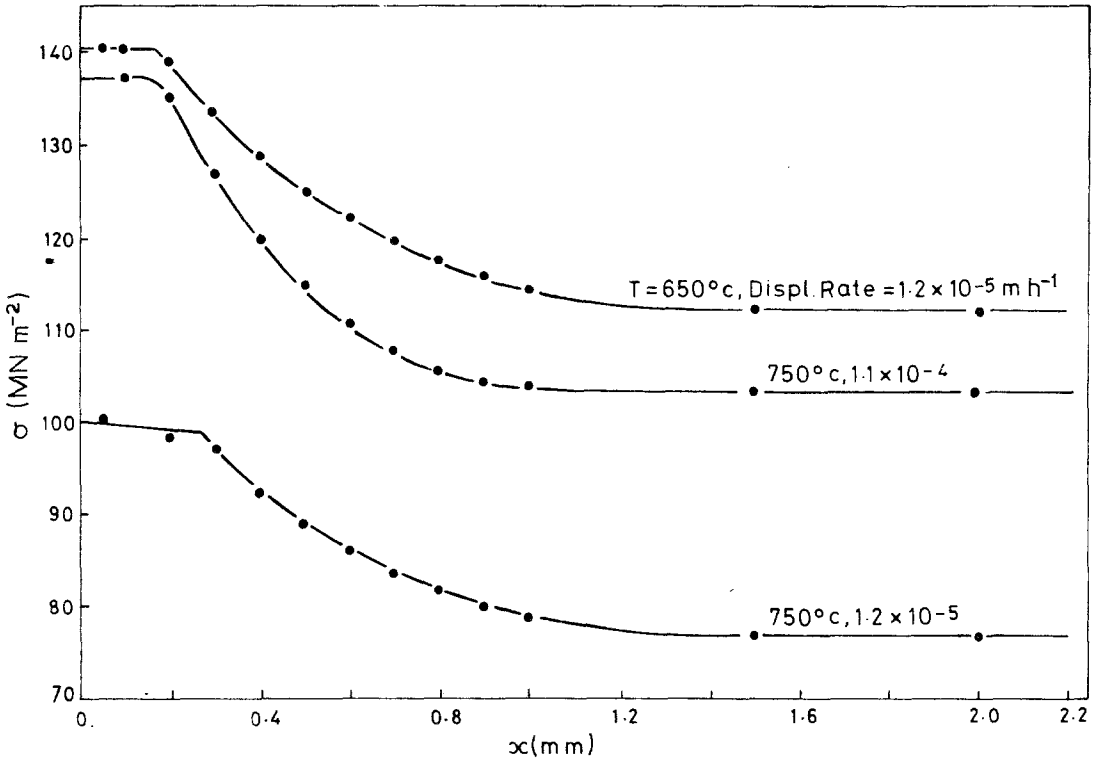

Figure 6 Crack tip stresses, derived from strain rates, as a function of distance from the crack tip x.

where m is previously determined from a series of plain bar tests. Thus the stress distributions of Fig. 6 were arrived at. The models of crack-tip stresses can be compared with this distribution graphically and by experimentally determining s where the experimental distribution is fitted to $\sigma_{ss} = Fx^{-s}$, F and s being constants determined by the applied stress and temperature. Fig. 7 shows the comparisons, though in making the comparison it is clearly necessary to omit the constant strain rate and stress region, taking the origin for the stress distribution to be at a distance R from the observed crack tip. This distance R deserved further investigation, but it does not seem to correspond to the reach of microstructural damage which appeared to be concentrated to within 120 μm of the crack tip whereas R was typically more than 0.1 mm. This is due to the strain gradient within distance R of the crack tip produced by stress relaxation before steady state conditions were established.

The comparison of Fig. 7 indicates that the $x^{-1/(m+1)}$ is a more successful description of the experimental results. Further, Table I shows the measured values of s compared with the models where $s = 1/2m$ and $s = 1/(m+1)$, where m is taken from plain bar tests. Clearly the experimental s value is much closer to $1/(m+1)$.

5. Discussion

The creep rate normal to the crack plane should be controlled by the local tension stress in that direction in the vicinity of a crack tip, since this is the local effective stress. Derivation of the local

TABLE I Comparison of experimental values of S with model predictions

Temp (° C)	Cross-head rate ($m h^{-1}$)	m plain bar tests	S exptl.	$S = \frac{1}{m+1}$	$S = \frac{1}{2m}$	R (mm)
750	1.2×10^{-5}	7.0*	0.175	0.125	0.071	0.3
750	1.1×10^{-4}	7.0	0.195	0.125	0.071	0.15
650	1.2×10^{-5}	9.5*	0.129	0.096	0.052	0.15

*Reference [9].

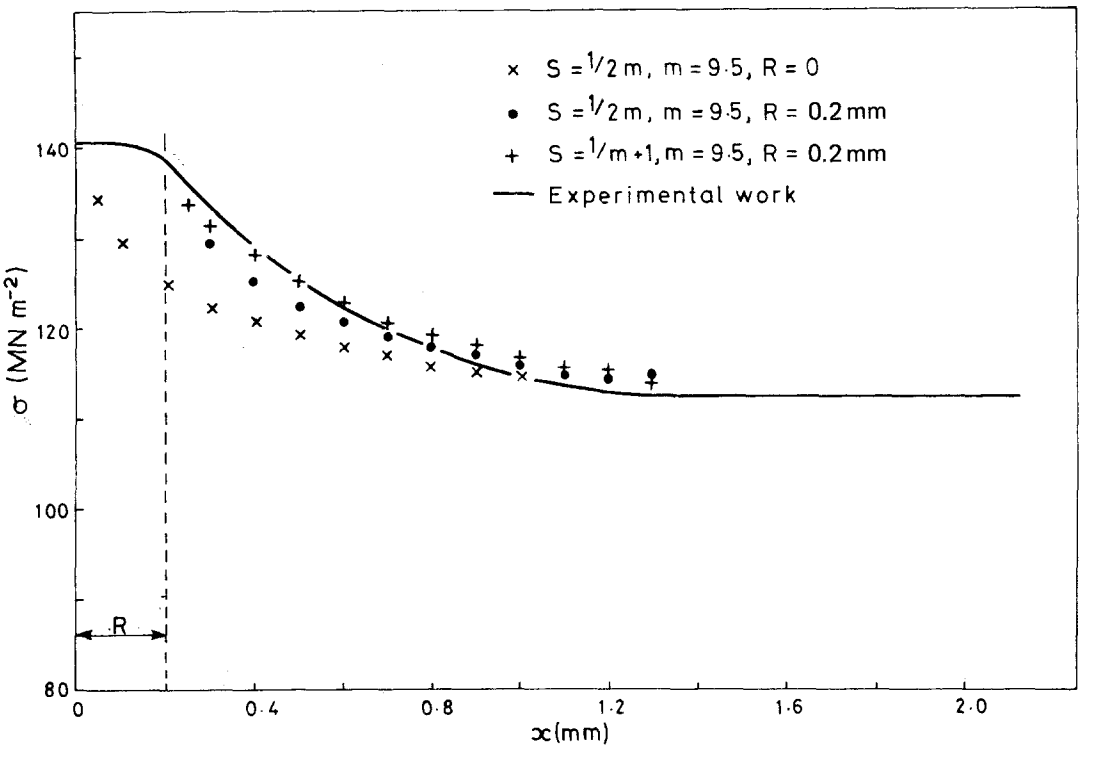

Figure 7 Steady state stress distribution derived from measured local strain rates, and compared with model predictions for test at 650° C and displacement rate $\dot{\delta} = 1.2 \times 10^{-5}$ m h^{-1}.

stresses from measured strain rates is therefore reasonable, though subject to the errors involved in the measurement of the exponent m. The stress distribution obtained in this way supports the $x^{-1/(m+1)}$ distribution. The experimental work is therefore further circumstantial evidence of a $1/x$ singularity in elastic strain energy density at a crack tip.

The constant strain rate, constant stress region R is not entirely unexpected behaviour since many factors would dictate unusual behaviour very close to the tip. The slit crack equations generally used [16, 17] are not applicable very close to the tip of a real crack which has a finite width and traction free surfaces. Further the microstructural damage, seen in these experiments as creep cavities distributed ahead of the crack tip, must give rise to extra redistribution of stresses to an unknown distance. The region R is therefore of considerable interest as far as the mechanism of crack advance is concerned and further work on this is a progress.

Appendix

Assuming crack-tip stress distributions can be obtained using Neuber's rule [18] by imagining the hypothetical elastic stress distribution to relax down the hyperbola $\sigma\varepsilon = \text{constant}$ to the point where it intersects the power law curve $\dot{\varepsilon} \equiv \varepsilon = A\sigma^m$, then the elastic stress $K/(2\pi x)^{1/2}$ decays to the steady state value

$$\sigma_{ss} = \left(\frac{K^2}{2\pi AE}\right)^{1/(m+1)} x^{-1/(m+1)}. \quad (1A)$$

Here K is the elastic stress intensity factor.

Taking this as the new near-tip distribution we now have to find the level of the distribution using an overall equilibrium requirement of an unchanged load carrying ability of the ligament.

Consider a single edge-notched tension specimen of gross width W, crack length a, thickness B, undergoing creep at constant load P. Then

$$P = B\int_0^{W-a} \sigma_{ss}(x)\,dx \quad (2A)$$

Using Equation 1A;

$$P = B\int_0^{W-a}\left(\frac{K^2}{2\pi AE}\right)^{1/(m+1)} x^{-1/(m+1)}\,dx \quad (3A)$$

or

$$P = B\left(\frac{K^2}{2\pi AE}\right)^{1/(m+1)}\left[\frac{m+1}{m}(W-a)^{m/(m+1)}\right] \quad (4A)$$

In Equation 4A the invalid assumption is that the near-tip distribution is continued right across the ligament. In linear elastic fracture mechanics (LEFM) a similar problem arises and is dealt with by adjusting the load-carrying capacity with a finite width correction factor. This factor can be modified for the redistributed σ_{ss} stresses as shown in [10]. Thus the K is modified to K' and the K' can be derived from the K-calibration curves used in LEFM. Incorporating this method Equation 4A becomes

$$P = B\left(\frac{K'^2}{2\pi AE}\right)^{1/(m+1)}\left[\frac{m+1}{m}(W-a)^{m/(m+1)}\right] \tag{5A}$$

Thus K' is given by

$$K' = (2\pi AE)^{1/2}\left[\frac{P}{BW}\frac{m}{(m+1)}\frac{W}{(W-a)^{m/(m+1)}}\right]^{(m+1)/2} \tag{6A}$$

Thus when $m \gg 1$, K' becomes

$$K' = (2\pi AE)^{1/2}\left[\frac{P}{BW}\frac{W}{(W-a)}\right]^{(m+1)/2}. \tag{7A}$$

Here the second term is clearly the net section stress to the power $(m+1)/2$.

Consider an element ahead of the crack tip where the local strain rate is given by

$$\frac{d\varepsilon}{dt} = A\left[\sigma_{ss}(x)\right]^m, \tag{8A}$$

or

$$\frac{d\varepsilon}{dt} = A\left[\left(\frac{K'^2}{2\pi AE}\right)^{1/(m+1)} x^{-1/(m+1)}\right]^m. \tag{9A}$$

If the strain arises from a displacement u over a small local gauge length L, then the local displacement rate is:

$$\frac{du}{dt} = LA\left[\left(\frac{K'^2}{2\pi AE}\right)^{1/(m+1)} x^{-1/(m+1)}\right]^m. \tag{10A}$$

We now assume that when u reaches a critical value, u_c at $x = d_c$, where d_c is a material property, then parting occurs and the crack advances. This is consistent with the crack opening displacement work of Wells and McBride [6]. The crack tip then moves at a rate da/dt proportional to du/dt such that

$$\frac{da}{dt} = \frac{du}{dt}\left(\frac{x}{d_c}\right)^{m/(m+1)};$$

that is

$$\frac{da}{dt} = LA\left[\frac{K'}{EA2\pi d_c^{1/2}}\right]^{2m/(m+1)}. \tag{11A}$$

Thus for the case of Newtonian flow, which is directly analogous to LEFM, $m = 1$ and $da/dt \propto K$, the growth rate is dependent on the elastic stress intensity factor. In contrast, for $m \gg 1$, then $da/dt \propto (\sigma_{net})^m$. Between these limits the behaviour can be described by

$$\frac{da}{dt} \propto (K')^{2m/(m+1)}.$$

This will represent the behaviour reasonably well until m rises sufficiently to make the net section stress correlation superior. As shown in [10], tests must cover a sufficient range of a/w to make the correlation apparent.

Experimental work has shown an apparent correlation between da/dt and K in the intermediate m range (i.e. $7 > m > 1$) of the form $da/dt \propto K^m$. It can be shown from the above analysis that such an apparent correlation can occur in this intermediate range. Equation 6A can be written as

$$K' = (2\pi AE)^{1/2}\left[\frac{P}{BW}\frac{m}{m+1}\frac{W^{1/2}}{(W-a)^{m/(m+1)}}\right]^{m+1/2}$$

$$= (2\pi AE)^{1/2}\left[K\frac{N(a)}{Y(a)}\right]^{(m+1)/2}$$

where

$$N(a) = \frac{m}{m+1}\cdot\frac{W^{1/2}}{(W-a)^{m/(m+1)}}.$$

In this intermediate range,

$$\frac{da}{dt} \propto K'^{2m/(m+1)}.$$

Substitution for K' in Equation 11A:

$$\frac{da}{dt} \propto \left[K\frac{N(a)}{Y(a)}\right]^m;$$

i.e. an apparent correlation between creep-crack growth rate and K^m.

References

1. J. A. WILLIAMS, *Phil. Mag.* **15** (1967) 1289.
2. N. G. NEEDHAM and G. W. GREENWOOD, *Met. Sci. J.* **9** (1975) 258.
3. F. K. G. ODQVIST, "Mathematical Theory of Creep and Creep Rupture" (Oxford University Press, Oxford, 1974).
4. I. W. GOODALL and E. J. CHUBB, CEGB Report RD/B/N3227 (1974).
5. J. A. WILLIAMS and A. T. PRICE, CEGB Report No. RD/M/R205 (1974).
6. A. A. WELLS and F. H. McBRIDE, *Can. Met. Quart.* **6** (1967) 347.
7. G. J. NEATE and M. J. SIVERNS, Proceedings of the International Conference on Creep and Fatigue in Elevated Temperature Applications, (Inst. Mech. Eng., 1974).
8. J. L. KENYON, G. A. WEBSTER, J. C. RADON and C. E. TURNER, *ibid.*
9. R. D. NICOLSON, Ph.D. thesis, University of Aston, 1975.
10. J. T. BARNBY, *Eng. Fract. Mechs.* 7 (1975) 299.
11. N. J. HOFF, *Q. Appl. Mater.* **12** (1954) 49.
12. Y. H. PAO and J. MARIN, *J. Appl. Mechs.* **20** (1953) 245.
13. J. E. SRAWLEY, Practical Fracture Mechanics for Structural Steel, edited by M. O. Dobson, (Chapman and Hall, London, 1969).
14. J. T. BARNBY, *Eng. Fract. Mech.* **6** (1974) 627.
15. R. D. NICHOLSON and C. L. FORMBY, *Int. J. Fracture* **11** (1975) 595.
16. J. R. RICE and G. F. ROSENGREN, *J. Mechs. Phys. Solids* **16** (1968) 1.
17. J. W. HUTCHINSON, *ibid* **16** (1968) 337.
18. H. NEUBER, *Trans. ASME, (J. Appl. Mechs.)* (1961) 544.

Received 18 October 1976 and accepted 22 February 1977.